

VISIBLE WAVELENGTH FREE ELECTRON OSCILLATOR

D. R. Shoffstall
Boeing Aerospace Company
Seattle, Washington

Abstract (U)

(U) The overall goal of the visible oscillator program is to demonstrate that a large FEL interaction strength can be obtained at approximately 600-nm wavelength. The gain-extraction product increases with increasing wiggler length, and a 5-m length with hybrid SmCo_5 technology was identified at the program start³ as providing satisfactory interaction strength, reasonable cost, and an acceptable extrapolation from previous wigglers. The 120-MeV LINAC comprises five accelerator sections, each powered by a 12-MW peak output RF klystron power station. The operating frequency is 1.3 GHz. The structure is a constant gradient traveling wave (TW), operating in the $3\pi/4$ mode. A TW design was chosen to accommodate the wide range of beam loading conditions required in the FEL experimental series. The radio frequency (RF) LINAC current format is a series of high-current micropulses spaced at the two way oscillator cavity transit time. The envelope of these pulses, the macropulse, is selected to be long enough to examine the laser startup and beam quality physics, nominally 100-200 μs .

1.0 Summary (U)

(U) The extension of free electron lasers (FEL) laboratory scale research dedicated to a deployed and fully operational weapon system requires significant advances in accelerator and laser technology. The power and wavelength scaling to a weapon size system entails critical technology risks and related issues. The Boeing Aerospace Company (BAC) with Strategic Defense Initiative Office (SDIO) and United States Army Strategic Defense Command (USASDC) concurrence, has mapped an incremental approach. The successful execution of this experimental series will prove the scientific feasibility, provide the critical technology and support the USASDC readiness to proceed with a medium-power FEL device demonstration at White Sands Missile Range (WSMR).

(U) This paper reports on the progress and status of the first incremental step.

2.0 Experimental Design and Configuration (U)

(U) The overall goal of the visible oscillator program is to demonstrate that a large FEL interaction strength can be obtained at approximately 500-nm wavelength. This interaction strength is properly measured in terms of the gain-extraction product^{1,2} and in this case, a design goal was chosen for 5% extraction with the available optical gain large enough for suitable oscillation startup and saturation within the macropulse length (100-200 μs nominal).

(U) The gain-extraction product increases with increasing wiggler length, and a 5-m length

(U) with hybrid SmCo_5 technology was identified at the program start³ as providing satisfactory interaction strength, reasonable cost, and an acceptable extrapolation from previous wigglers. With the assumption of a wavelength and wiggler length, an optimization analysis assuming a perfect electron beam (no energy spread or emittance) shows that approximately 100-MeV energy and a 2-cm period are required. The incorporation of realistic emittance and energy spread values modify this result, and a detailed calculation of the available gain for various⁴ electron beam qualities is shown in figure 2.1. Each curve is drawn under the assumption that the wiggler is optimized for the particular conditions at that point.

(U) The shift in optimum operating point with changing electron beam quality is seen in figures 2.2 and 2.3. In figure 2.2, the trend to larger e-beam energy with increasing emittance is observed. This shift results from the sensitivity to off-axis electrons being dependent on the wiggler wavelength. The design point of figure 2.2 is purposefully chosen to slightly higher than optimum energy for the expected 0.01-cm-rad emittance, to reduce the gain loss if slightly larger emittances are encountered. The importance of designing the system for the particular emittance expected is shown dramatically in figure 2.3. Here the gain fall off as a function of emittance is shown for three separate designs, each optimized for a different emittance. The performance at 0.01 cm-rad is quite poor for the zero emittance design, but for operation at 0.01 cm-rad with the 0.01-cm-rad design, the gain is substantially larger.

(U) The basic parameter set for the electron beam, wiggler, and optical cavity is shown along with the fundamental laser parameters in figure 2.4. The combination of 100-A peak current and the 5-m tapered undulator produce a small signal gain of 20% and a saturated gain of 10%. The extraction at saturation is 5%. Higher gains are available at reduced taper and extraction. The 55-m optical cavity length is determined directly by the required extraction and available gain. The mirrors are separated from the wiggler to the point at which the macropulse average incident intensity of 300 kW/cm². This operating point for the mirrors is estimated to be within the capability of the dielectric coatings, based on related measurements at Los Alamos National Laboratory (LANL)⁵.

(U) The Physical Sciences Center at Boeing has been enlarged to accommodate the accelerator and laser. The experimental configuration is shown in figure 2.5. The facility size is roughly 12 m x 70 m.

3.0 RF LINAC (U)

(U) Accelerator Design. The 120-MeV LINAC

(U) comprises five accelerator sections, each powered by a 12-MW peak output RF klystron power station. The operating frequency is 1.3 GHz. The structure is a constant gradient traveling wave (TW), operating in the $3\pi/4$ mode. A TW design was chosen to accommodate the wide range of beam loading conditions required in the FEL experimental series. The radio frequency (RF) LINAC current format is a series of high-current micropulses spaced at the two way oscillator cavity transit time. The envelope of these pulses, the macropulse, is selected to be long enough to examine the laser startup and beam quality physics, nominally 100-200 μ s. As a consequence of this long macropulse requirement, the susceptibility of the accelerator waveguide to beam breakup becomes a major issue. To address this problem, the structure has innovative features to mitigate the influence of dipole cavity modes and transverse wakefields. Synchronous interaction of the beam with transverse electromagnetic modes is minimized in $3\pi/4$ mode structure since TM_{11} -like modes do not propagate at the velocity of light⁶. In addition, since the transverse modes have a negative group velocity, they can be removed from the structure at the upstream end of the waveguide. This is accomplished by routing the higher modes through the input RF coupler to a resistive, probe loaded coaxial pipe.

(U) Transverse wakefield effects which can degrade emittance of high-charge micropulses are strongly dependent on the disk aperture diameter. A large aperture structure with acceptably low group velocity is achieved with thick disks. Shunt impedance is enhanced by contouring the disk nosecones and coving the cavities. The resultant apertures range from 5-7 cm, roughly three times the size used in our S-band Stanford Linear Accelerator Center (SLAC)-like prototype accelerator.

(U) Measurements of beam induced cavity modes have been performed for candidate structure designs. These tests⁷ show significant transverse mode reduction in the design structure.

(U) Figure 3.1 is a schematic drawing of the acceleration guide. The electrical characteristics are given in figure 3.2.

(U) The electric field strength at 12-MW input is 9.9 MV/m and the section no-load energy gain is 29.1 MeV. The full accelerator load line and FEL operating point are given in figure 3.3.

(U) Injector. A two stage subharmonic injector for the 120-MeV LINAC has been designed and tested with the existing S-band accelerator. Single microbunch output beam current of 120A with emittance of 0.008 cm-rad and energy width of 1% has been measured^{8,9}.

(U) The subharmonic injector, figure 3.4, consists of a high-current triode gun, two standing wave cavity prebunchers and a fundamental frequency tapered phase velocity buncher. A "pepper pot" emittance measurement and tuning diagnostics occupy the space between

(U) the prebuncher cavities. A full solenoidal magnetic field provides radial containment and focusing of the electron beam. A tapered collimator in the last drift section limits beam size and entry angle at the buncher.

(U) The electron source is similar to the SLAC-collider injector gun design. This gun provides a high brightness output and the relatively low grid drive voltage is advantageous for our requirement of high repetition, nanosecond pulse gating.

(U) RF Power Stations. Installation and testing of the 1.3-GHz RF power stations for the FEL oscillator experiment have been completed. Each of these stations was tested to the following specifications.

RF Power	15 MW	10 MW
RF Pulse Width	150 μ s	300 μ s
RF Average Power	50 kW	50 kW

(U) A drawing of the RF power station is shown in figure 3.5.

(U) The RF power supply circuit is divided into three subassembly cabinets:

- a. (U) The high-voltage dc power supply is a 30-kV, 10 average, SCR-regulated supply with soft start voltage programming and an automatic load over-current trip with 8-ms response time to isolate the power supply from the mains.
- b. (U) The regulator circuit includes the filter capacitors, a 2H air-core resonant charging choke, and a floating deck de-Q regulator. The circuit regulation is 1%. The air-core choke prevents high-current faults from load shorting.
- c. (U) The modulator circuit includes the 52-coil, 52-capacitor, 300 μ s, 10-ohm pulse-forming line; the output thyatron switch; and the line and load protection circuitry. The power supply control electronics are also located in this enclosure.

(U) The power supply average power is upgradable to 100 kW with a replacement thyatron, all other components are full 100 kW RF rated.

(U) The supplies are fully computer controlled, with fiber optic linkage to the main control room for electrical noise immunity.

(U) Thomson-CSF has developed a new long pulse L-band klystron designated as TH2104 for the FEL series. Six of these tubes have been procured. All tubes were delivered on time and all have fully met or exceeded our operating requirements. A configuration drawing and the performance specifications for the TH2104 klystron are shown in figure 3.6.

4.0 Beamline (U)

(U) The FEL electron beam transport system is composed of three sections, as shown in figure 4.1. The beam from the accelerator enters the

(U) first section, a quadrupole focus-drift-defocus-drift (FODO) array, which measures beam and transports the beam to the second section, a 180-deg bend, where beam energy and emittance are tailored. The third section focuses and steers the beam into the wiggler.

(U) The beamline contains several diagnostic and tuning aids, which include fluorescent screens, collimators, energy slits, and steering coils. A spectrograph is located after the wiggler for examining energy spectra during low-power tuning. In addition, 25 stripline detectors are located along the length of the beamline. Energy selection slits are located at two points in the center of the diagonal legs of the 180-deg bend where the energy dispersion is the highest. The principal electron beam diagnostic measurements for the FEL experiment are shown in figure 4.2.

(U) Collimator holes are incorporated at the beginning and the end of the first FODO array. A third collimator is located in the center of the 180-deg bend. Steering coils are located all along the beamline. These coils serve as a tuning diagnostic and a steering corrector. The beamline is now completely assembled and operational.

5.0 Wiggler (U)

(U) The FEL experiment wiggler is a 5-m variable taper permanent magnet device. The magnetic circuit uses samarium cobalt magnetic material and vanadium permendur pole pieces. The wiggler was designed and built by Spectra Technology, Inc (STI). STI has named the wiggler THUNDER (for tapered hybrid undulator).

(U) The THUNDER wiggler has been designed to provide the high interaction strength required for efficient laser operation at visible wavelengths. The 10 kG magnetic field, roughly three times higher than that of previous 10- μ m experiments, together with a 5-m overall length, provide 10% optical gain at 5% electron energy extraction. The high field is achieved with a hybrid design in which samarium cobalt permanent magnets drive vanadium permendur poles. This geometry allows higher field strengths for a given gap-to-wave-length ratio than possible with pure samarium cobalt designs. The hybrid design is also chosen because the steel pole pieces provide improved field uniformity and, therefore, better electron transport. The transport issue becomes increasingly critical at short wavelengths with the small optical beam size, and to further reduce field errors, the magnets and wiggler structure are dimensionally and positionally controlled to less than 0.001 inch. The system employs two-plane electron beam focussing by means of pole canting. This canting imposes a quadrupole field component which adds focussing in the plane of the wiggler while reducing the natural focussing in the orthogonal plane. Such two-plane focussing was unnecessary in earlier 10- μ m experiments.

(U) The wiggler is built in ten 50-cm segments, which can be seen just prior to final assembly in figure 5.1. The magnetic gap is manually adjustable by choice of a precision

(U) ground spacer block. This allows variation of the energy taper from 0 to 12%.

(U) At either end of each 50-cm segment resides a compact diagnostic station (figure 5.2). A "pop-in" target, which is either a fluorescent screen or the Cherenkov cell, provides visual information on the profile and size of the electron beam with respect to the alignment laser beam that also is imaged on the screen. Additionally, stripline electrode beam position monitors are provided. These striplines are mounted on the tips of the poles of the steering elements to conserve space. The design resolution of the striplines is better than the requirement of 30 μ m.

6.0 Optical Cavity (U)

(U) The optical cavity for the visible oscillator experiment placed unusually high demands on both fabrication and alignment of the spherical cavity mirrors. It was important to fabricate the mirrors so that the Rayleigh range and the mirror spacing were fixed to a value predetermined by the wiggler size and the micropulse interval. When reduced to figure requirements, the mirror radius had to match an absolute radius to within approximately $\lambda/50$.

(U) Damage limitations required a spot size of at least 1 cm on the end mirrors; to accommodate the 5-m long wiggler, a Rayleigh length of 2.4m was chosen. This dictated a cavity that is approximately 60m from end mirror to end mirror. The actual length chosen was 55.4m to provide a cavity round-trip time equal to the micropulse spacing.

(U) The mirrors themselves are 4 in. in diameter and 1.5 in. thick. The FEL beam illuminates the central portion only, and the remainder of the mirror is used for the stabilization system. Fused silica was chosen as the mirror material for several reasons: it can be polished to a supersmooth surface; which is necessary for damage resistant coatings; it has a low coefficient of thermal expansion so that small changes in temperature throughout the structure of the mirror have little effect on the figure of the mirror; and it is transparent to the FEL light, which is important since we are outcoupling light through the cavity end mirrors.

(U) Once in place, 55.4m from each other, the mirror must be aligned and stabilized to better than 50 nanoradians. To accomplish this, a servo controlled stabilization system was designed and built. The heart of the system is the voice-coil driven, active optical mount shown in figure 6.1, and the analog electronics which command it. The system has been built, installed and tested. It provides active stabilization of each mirror to a few tens of nanoradians with a bandwidth of 200 Hz. Initial alignment of the system is done by injecting an on-axis laser light and maximizing the containment time for that light.

(U) All components of the optical system have been built, tested and installed. The system reached initial operational status in July 1986.

References (U)

- 1 J. M. Slater, IEEE J. Quantum Elect., "Tapered-Wiggler Free Electron Laser Optimization", Vol. GE-17, 1981, pp. 1476-1479.
- 2 J. L. Adamski, T. L. Churchill, W. M. Grossman, R. C. Kennedy, D. C. Quimby, D. R. Shoffstall, J. M. Slater, Workshop on FEL, "Demonstration of Large Electron Beam Energy Extraction by a Tapered Wiggler FEL", 1983, Orcas Island, WA, June 1983.
- 3 D. C. Quimby and J. M. Slater, 1983 Workshop on Free Electron Lasers, "Emittance Acceptance in Tapered-Wiggler Free Electron Lasers", Orcas Island, WA, June 1983.
- 4 D. C. Quimby, and J. M. Slater, IEEE J. Quantum Elect., "Electron-Beam Requirements for Tapered-Wiggler Free Electron Lasers", Vol. GE-21, 1985, pp. 988-997.
- 5 Free Electron Laser Program Kickoff Meeting, Los Alamos, NM, Jan 3-Feb 1, 1984.
- 6 W. J. Gallagher, Particle Accelerators, "Periodic Transmission-Line Mode Measurements", Vol. 16, 1984, p. 113.
- 7 J. L. Adamski, W. J. Gallagher, A. M. Vetter, Paper Q19, the Conference, "Observation of Beam-Excited Dipole Mode in Traveling Wave Accelerator Structure".
- 8 J. L. Adamski, W. J. Gallagher, R. C. Kennedy, and A. D. Yeremian, IEEE Trans. Nuc. Sci., "A High Current Injector for the Boeing Radiation Laboratory FEL Experiment", Vol. NS-30,4, Aug. 1983, p. 2696.
- 9 J. L. Adamski, W. J. Gallagher, R. C. Kennedy, D. R. Shoffstall, E. L. Tyson, A. D. Yeremian, Paper D43, the Conference, "The Boeing Double Subharmonic Electron Injector - Performance Measurements".

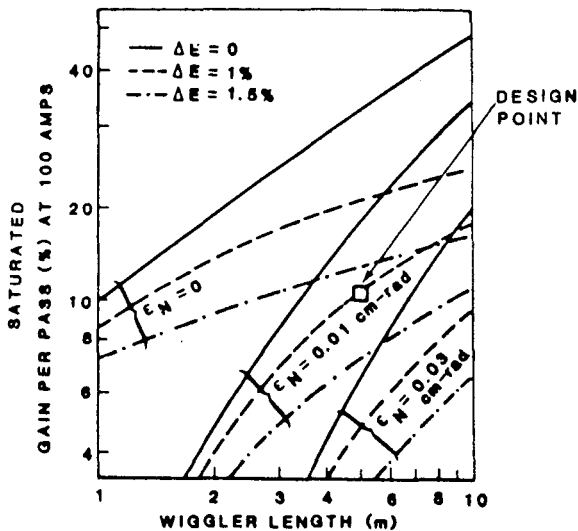


Figure 2.1 Calculated Optical Gain

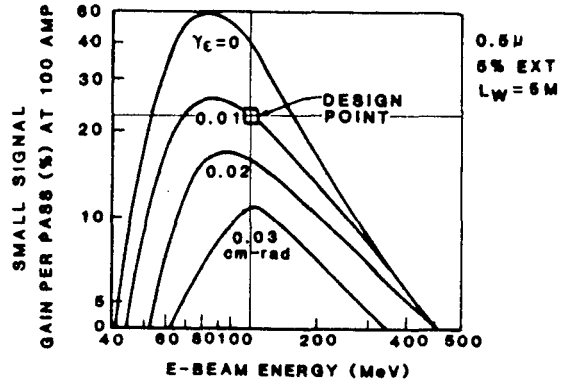


Figure 2.2 Calculated Optical Gain

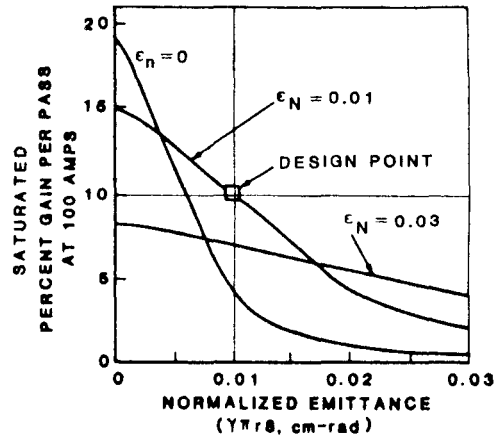


Figure 2.3 Calculated Optical Gain

LINAC	WIGGLER
<ul style="list-style-type: none"> • E = 120 MeV • i_{peak} = 100A • $\epsilon'_N = \gamma\pi r\theta$ = 0.01 cm-rad • $\Delta\gamma/\gamma$ = 0.01 FW 	<ul style="list-style-type: none"> • LENGTH = 5m • WAVELENGTH = 2.18cm • PEAK FIELD = 10.2kG • TAPER (ENERGY) = ADJUSTABLE TO 12%
OPTICAL CAVITY	LASER
<ul style="list-style-type: none"> • LENGTH, 55m • SPOT SIZE W, 1cm AT MIRROR, 0.5mm AT CENTER • MIRROR LOADING, 300kW/cm² AT MAXIMUM EXTRACTION 	<ul style="list-style-type: none"> • GAIN: SMALL SIGNAL 20% SATURATED (AT 8GW) 10% • EXTRACTION AT 8GW: 5% (12% TAPER) • MACRO POWER, 30kW

Figure 2.4 System Design Parameters

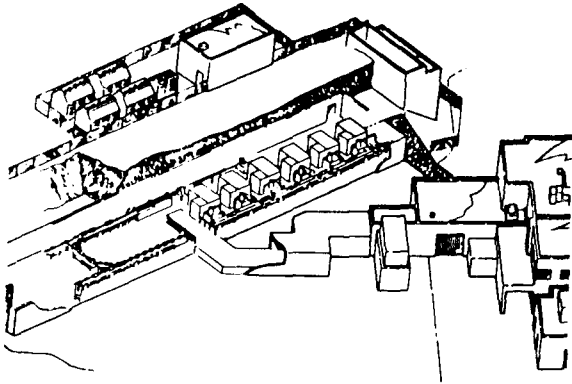


Figure 2.5 Visible FEL Experiment

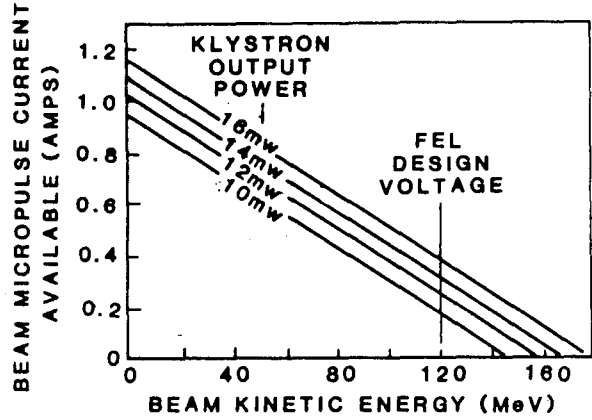


Figure 3.3 Accelerator Load Line

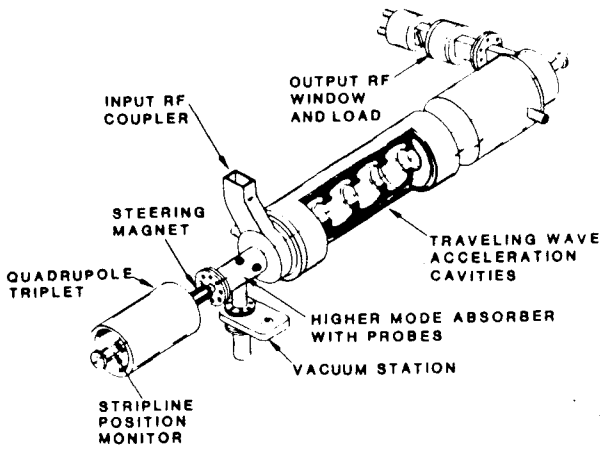


Figure 3.1 Accelerator Waveguide Section

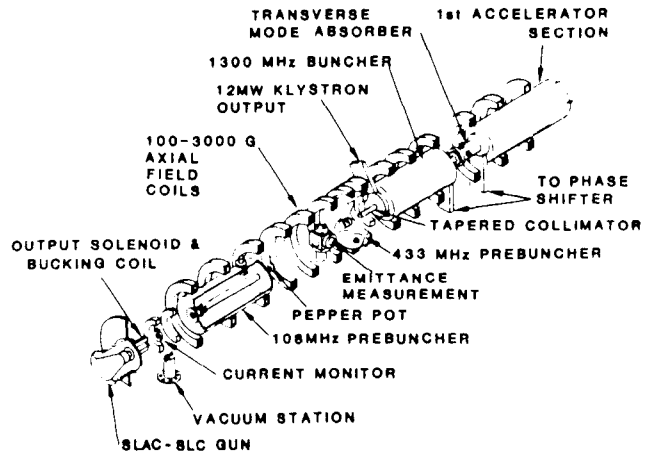


Figure 3.4 Two-Stage Subharmonic Injector

NOMINAL OPERATING FREQUENCY f	= 1300 Mcs ($\nu_p - c$)
DESIGN INDEX (ATTENUATION) $2I_0L$	= .6 NEPERS (4dB)
INITIAL ATTENUATION COEFFICIENT, I_0	= .102 NEPERS/m
WAVEGUIDE LENGTH, L	= 2.94m
SHUNT IMPEDANCE PER UNIT LENGTH, r	= 40 MEGOHMS/m
FIGURE OF MERIT, Q	= 20,200
INITIAL NORMALIZED GROUP VELOCITY, v_g/c	= .0087

Figure 3.2 Accelerator Structure Design Parameters

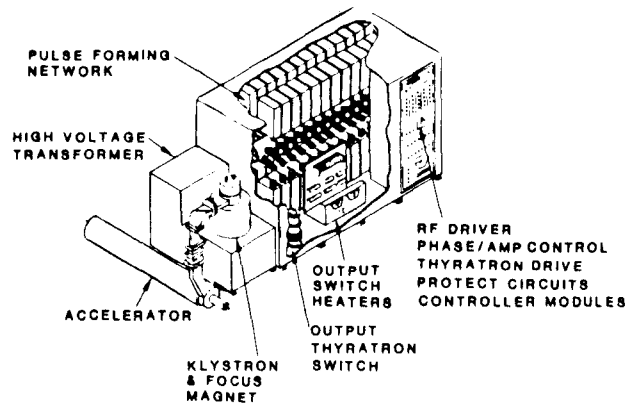
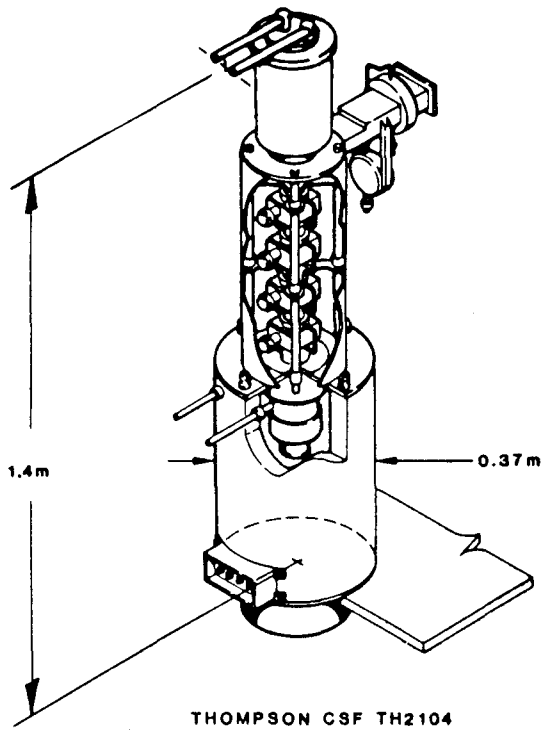


Figure 3.5 RF Power Station



TH2104 KLYSTRON OPERATING SPECIFICATIONS	
● FREQUENCY, MHz	1300
● PEAK POWER, MW	10 - 15
● AVERAGE POWER, MW	0.1 - 0.05
● PULSE DURATION, ms	0.2 - 0.1
● CATHODE VOLTAGE, kV	185 - 215
● CATHODE CURRENT, A	160 - 200
● HEATER VOLTAGE, V	25
● HEATER CURRENT, A	25
● EFFICIENCY (MINIMUM), %	38
● GAIN AT SATURATION, dB	60
● INSTANTANEOUS BANDWIDTH, MHz	8
● LOAD VSWR (MAXIMUM)	1.5
● SOLENOID, kW	10

Figure 3.6 FEL Klystrons

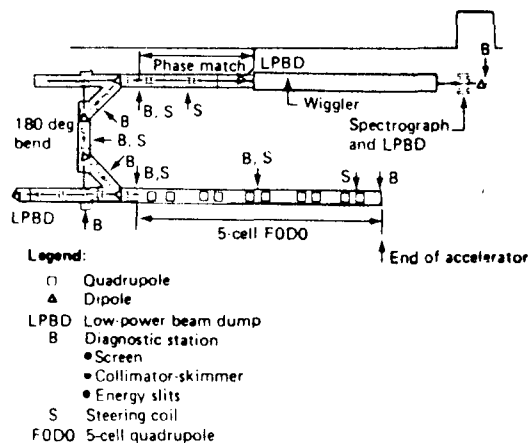


Figure 4.1 FEL Electron Beam Transport System

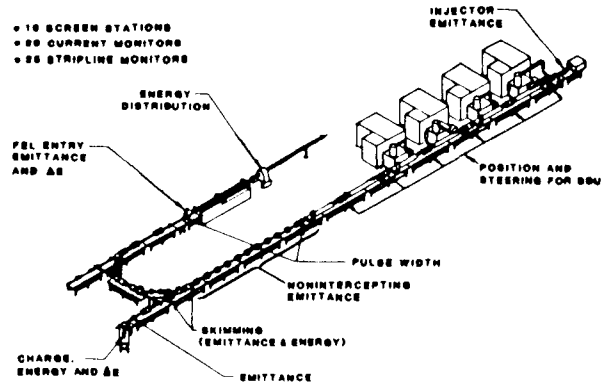


Figure 4.2 FEL Experiment Electron Beam Diagnostic Measurements

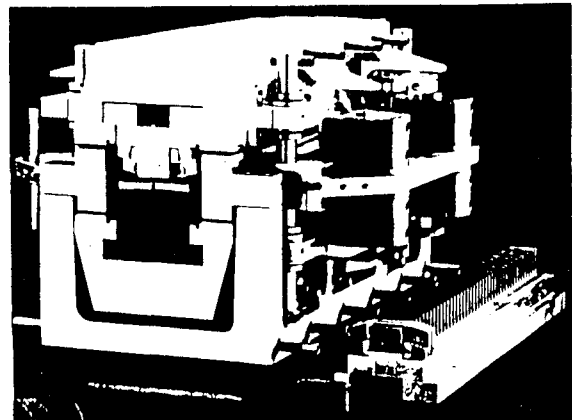


Figure 5.1 THUNDER Wiggler Section

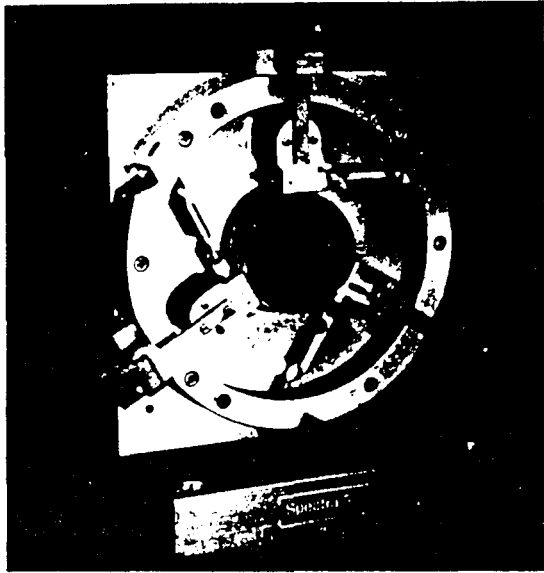


Figure 6.1 Mirror and Voice-Coil Driven Flexure Mount

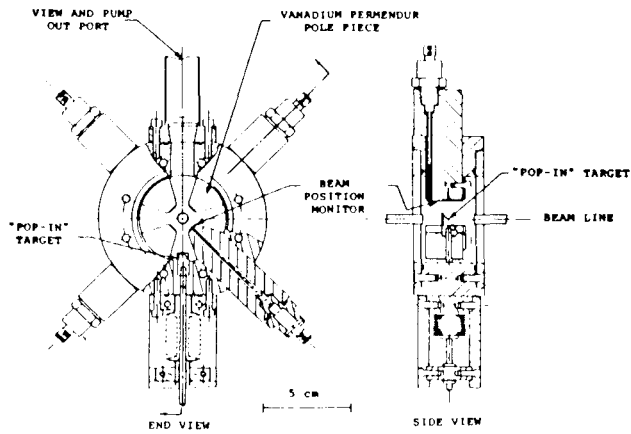


Figure 5.2 Wiggler Diagnostics